

Fuel Efficient High-Density Platooning Using Future Conditions Prediction

GUILLAUME JORNOD¹, ANDREAS PFADLER^{2,3}, SOFIA CARREIRA⁴,
AHMAD EL ASSAAD⁵, AND THOMAS KÜRNER¹ (Fellow, IEEE)

¹Institut für Nachrichtentechnik, Technische Universität Braunschweig, 38106 Braunschweig, Germany

²Autonomous Driving Department, Volkswagen Commercial Vehicles, 38440 Wolfsburg, Germany

³Network Information Theory Department, Technische Universität of Berlin, 10623 Berlin, Germany

⁴Instituto Superior Técnico, Universidade de Lisboa, 1649-004 Lisbon, Portugal

⁵Autonomous Driving Department, Volkswagen AG, 38440 Wolfsburg, Germany

CORRESPONDING AUTHOR: G. JORNOD (e-mail: guillaume.jornod@pm.me)

This work was supported in part by the Federal Ministry of Education and Research of the Federal Republic of Germany (BMBF) in the framework of the Project 5G NetMobil under Grant 16KIS0681.

ABSTRACT A promising application of cooperative driving is high-density platooning, which main goal is to reduce fuel consumption by driving with inter-vehicle distances below ten meters. The prediction of factors influencing the platoon capability to drive with such inter-vehicle distances the derived safe inter-vehicle distances, drives the potential fuel saving. Our aim is to study the influence of the prediction, especially the prediction horizon, on the achieved fuel saving as a function of different maneuver parameters. The contributions of this paper are: introducing the concept of maneuver reference to distribute the effort of maneuvering in truck platooning; linking the fuel consumption to a compensation time, that is the time during which the platoon will counterbalance the fuel consumption by benefiting from the reduced air drag; presenting an optimization method for maximizing the fuel saving depending on some predictive quality of service parameters. To model the fuel consumption and the duration of the maneuvers, we use a lasso regressions on data obtained from simulation. We then use these regression models in our optimization framework, which is based on particle swarm optimization. We show that to benefit from high-density platooning, the magnitude order of the prediction horizon required by a five-truck platoon is minimum hundred seconds.

INDEX TERMS Intelligent vehicles, vehicular ad hoc networks, optimisation, cooperative systems.

I. INTRODUCTION

An interesting and promising application of cooperative driving is high-density platooning (HDPL). Aiming to reduce their fuel consumption, vehicles, generally trucks, in a HDPL drive small inter-vehicle distances (IVDs)—15, 10 or even 5 m. Indeed, this reduction can be achieved thanks to reduced air drag [1]. In recent years, truck platooning aiming for energy efficiency has gained a lot of

attention in the field of cooperative vehicle automation research [2].

To achieve this efficiency whilst guarantying safety, the application requires the exchange of information with low latency and high reliability. The coordination between the vehicles is supported by vehicle-to-vehicle (V2V), or vehicle-to-everything (V2X) communications more generally. Safety-related time-critical applications tend to be limited by the lower-bound quality of service (QoS)—measured with key performance indicators (KPIs) such as packet error rate (PER), latency, data rate and packet inter-reception time (PIR)—of their communications systems [3]. In HDPL, this

The review of this article was arranged by Associate Editor Margarida Coelho.

limitation affects the IVD allowed for the trucks, and therefore on the achievable fuel saving. This impact of QoS on fuel saving is highlighted by [4] in their review of fuel economy for platooning. It is furthermore observable from the fact that most fuel efficiency studies assume a stable or a perfect communication link (e.g., [5], [6]). Effort for mitigating the delays has also been put in developing robust platooning control strategies, such as the distributed consensus strategy presented in [7].

Varying QoS is one example of a factor affecting the platooning vehicles to drive with low IVDs. Other examples are the traffic density and the presence of ingress and egress lanes. QoS is the main focus of the research project, 5GNetMobil, in which scope this work has been conducted. The predicted QoS is assumed to have been translated into a future safe IVD. The relationship between the two parameters, QoS and IVD has been studied in our previous work [8] for one QoS indicator, the PIR, which importance for automotive applications has been demonstrated in [9]. Using safe IVD instead of a QoS indicator allows us generalize the problem of fuel saving optimization in truck platooning. Indeed, the safe IVD could, in the future, be derived from a combination of road maps including ingress and egress lanes, instantaneous traffic information and radio parameters prediction, allowing to precisely determine the capability of a platoon to safely reduce the distance between the trucks in time and space. QoS is here used as an example as it is varying in a smaller time scale as traffic and is less predictable than ingress and egress lanes.

In [10], a method for computing optimal plans is proposed. It considers fuel-efficiency on the route level, providing optimal *rendezvous* points to decrease the fuel consumption. In [11], a multi-objective optimization method for platooning control is presented. It comprehensively encompasses vehicle safety, passenger comfort, formation control and fuel economy. In [12], the speed is planned with respect to the slope of the driven road while accounting for string stability. [13] presents an optimization problem also considering the slopes. The problem is based on distributed model predictive control (DMPC) and solved with particle swarm optimization (PSO). In [14], a method for providing the optimal speed profile is proposed. It takes the topography of the road and safety into account to improve the fuel efficiency of the platoon. None of these approaches consider the maneuvering times in the fuel consumption optimization. In the scope of predictive quality of service (PQoS), or generally with predicted influencing factors, these times have a large influence on the net fuel consumption.

In our previous work, we studied the impact of various external factors on the performance of HDPL supported by different radio access technologies. These factors are the number of surrounding nodes and the inter-antenna distance in [15], and the Doppler shift originating from incoming traffic in [16], [17]. These previous studies motivate the development of strategies for the adaptation to QoS variation. The prediction algorithm that provides the PQoS

could run on a base station, or be running on the nodes. In [18], we presented an algorithm for such decentralized QoS prediction; this algorithm can be used to provide the prediction of future conditions required as input for the method presented in the present paper. Part of the content of this paper is based on the fuel saving study presented in [19].

In this paper, we investigate the minimization of the fuel consumption given a minimum safe IVD and its availability period. This is achieved by studying the relationship between the control strategy and the objective of our system, the minimization of the fuel consumption. This metric is computed from the trigger of the IVD adaptation to the achievement of the maneuver, *viz.* when the target IVD is reached, that is encompassing the closing and the opening maneuver. To support these maneuvers, we present a concept for group control, the relative reference for the maneuver, along with other relevant control parameters. The maneuver reference concept extends the graph-based Laplacian control algorithm presented in [20] for the closing and opening maneuvers. We perform simulations using SUMO [21] and ns-3 [22], as we intend to use the developed strategies in the scope of simulations including a QoS prediction module.

We adapt the fuel consumption model of SUMO (see Section III-B.2 to reflect the air drag reduction. We derive the relationship between the fuel consumption and the duration of the chosen maneuver. The latter being of interest because it is a time during which the platoon saves less fuel. Using the air drag corrected fuel consumption model, we translate the fuel consumption investment in a compensation time. The resulting sets of maneuvering time and compensation time for the two maneuvers allow us to perform fuel saving optimization depending on the available prediction parameters.

The key contributions of this paper are:

- 1) Extending the distributed graph-based feedback convoy controller for closing and opening maneuvers by introducing the reference of the maneuver;
- 2) Introducing a compensation time that is translating the fuel consumption in a time that can be added to maneuver durations;
- 3) Presenting the optimization of the fuel saving depending on the future safe IVD values.

The remaining of this paper is organized as following. After introducing the used control model in Section II, we present the method employed to evaluate the relationship between fuel consumption and maneuvering time for HDPL in Section III. The simulation setup is also presented in this section, together with the simulated scenarios and some selected results. Section IV builds upon these results to provide an optimization framework for enabling fuel saving. Finally, this article is concluded in Section VI.

II. CONTROL STRATEGY

We aim at providing a fuel-efficient approach for HDPL using PQoS. An important feature for this approach is

the development of a control strategy for the IVD adaptation maneuvers. In this section, we present the platooning control strategy together with the input parameters for the optimization problem. The control strategy has three independent features: (i) the platooning controller, (ii) the local controller and (iii) the command input verification.

A. PLATOONING CONTROL ALGORITHM

For this study, we extend the longitudinal controller presented in [20] for IVD adaptation in terms of maneuver time and fuel efficiency. The advantage of this control strategy compared to classical cooperative adaptive cruise control (CACC) is that the formation is more robust to unstable communication links. A first study of the requirements on the communication system using this control strategy for emergency braking is presented in [23].

This distributed control algorithm is based on the Laplacian control principle [24]. Each vehicle computes its target speed using the following equation:

$$\dot{s} = -\mathcal{L}(s - \mathbf{b}) + \mathbf{v}_g, \quad (1)$$

where s is the position vector in the curvilinear coordinates frame following the displacement of the vehicle of interest, \mathbf{b} the bias vector that defines the formation and \mathbf{v}_g a vector composed of the scalar target group speed. s and \mathbf{b} are typically vectors of lengths in m and \mathbf{v}_g in m/s. The target speed is therefore expressed as the time derivative of the position vector, \dot{s} . \mathcal{L} is the Laplacian matrix, defined as:

$$\mathcal{L} = \mathcal{I} \cdot \mathcal{W} \cdot \mathcal{I}^T, \quad (2)$$

where \mathcal{I} and \mathcal{W} are, respectively, the incidence and the weight matrices of the graph composed by the vehicular ad hoc network (VANET). The nodes of this graph are the vehicles, and its edges the communication links.

The enhancement presented in this section consists of the offset and bias mechanisms. In the original algorithm presented in [20], the offset and bias are calculated with respect to the front vehicle, which is the reference of the maneuver. This definition is appropriate for the creation and the maintenance of the convoy. When it comes to the modification of the IVD, it is interesting to optimize the position of this reference point depending of the maneuver performed—increasing or decreasing the IVD—, aerodynamics parameters and the optimization objective. Indeed, on the one hand, having the reference in the middle of the platoon divides by two the maneuvering time. On the other hand, it is more efficient in terms of fuel consumption to have it behind when decreasing the IVD and in the front when increasing it. The introduced maneuver reference operates in the calculation of the offsets and biases.

Fig. 1 illustrates simple examples of combination of objectives and maneuver references for the closing maneuver. The represented maneuver references are the back, middle and front references. The latter corresponds to the classical CACC implementation, where the front vehicle is the

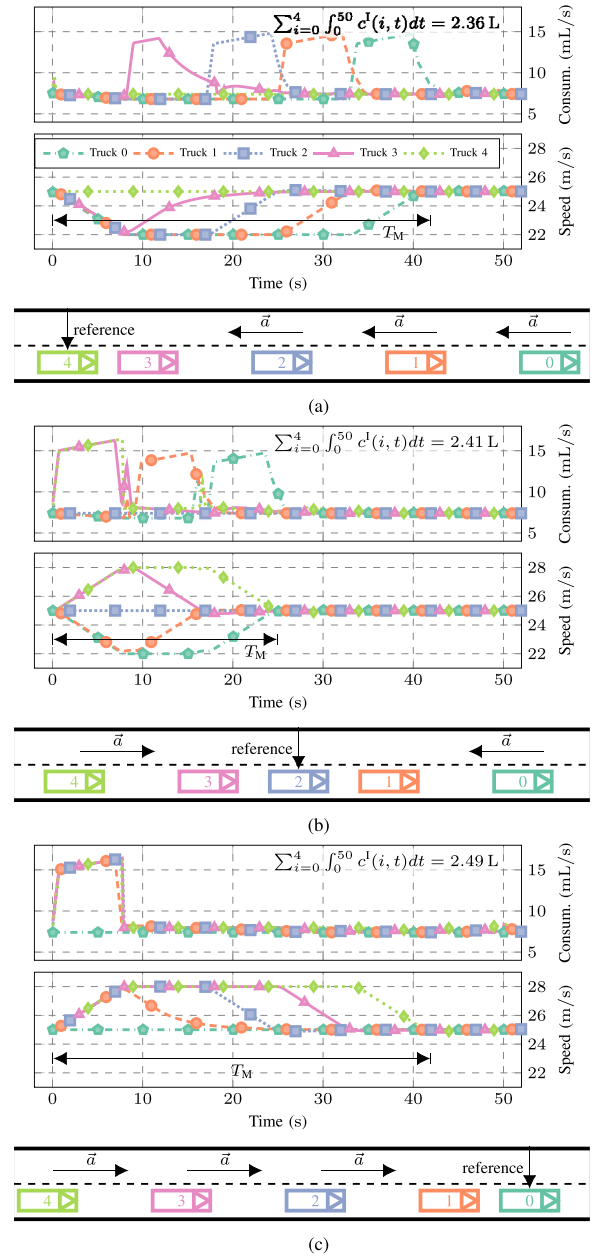


FIGURE 1. Reference placement for (a) fuel consumption optimization with reference in the back, (b) maneuver duration optimization with reference at the center, compared to (c) classical reference in the front during an IVD closing maneuver. For each reference example, the figure comprises the fuel consumption time series, the speed time series and an illustration of the reference influence on the maneuver. In the fuel consumption time series, plain curves represent the instantaneous consumption without air drag consideration. The overall consumption of the platoon over the 50 s experiment is also given in the top right corner. In the speed time series, we indicated the maneuvering time T_M . In the reference illustrations (third for each subsection), the direction of driving is from left to right and the horizontal arrows represent the direction of the acceleration.

reference of the formation maintenance. Using the back vehicle as reference, although the acceleration and deceleration seems to be symmetrically swapped, the overall fuel consumption is reduced compared the front reference, as the vehicles accelerate from 22 m/s to 25 m/s instead of 25 m/s to 28 m/s. Due to the symmetry in terms of maneuver

reference placement, the maneuver time remains the same. When the maneuver position is placed on the middle vehicle, the maneuver duration is halved and the fuel consumption slightly reduced compared to the front reference. The maneuver duration is reduced as the maximum travelled distance during the maneuver is also halved, thanks to the displacement of the reference. In this configuration, two trucks are also accelerating from a lower speed, as in the back reference, thus reducing the fuel consumption.

For the sake of simplicity, we only consider homogeneous target IVDs and vehicles within the platoon. In terms of platooning control, introducing heterogeneity in IVD or vehicle length would alter the symmetry of the formation and therefore the optimal placement of the maneuver. However, the characteristic of the vehicle fuel consumptions would also change and drastically increase the complexity of the optimization problem.

B. PARAMETERS

The platooning controller, which enables the group behavior, is described in Section II-A. The local controller translates the speed received from the platooning controller into an acceleration command. Finally, the command input verification ensures that the speed and acceleration commands do not infringe the dynamics constraints.

1) INTER-VEHICLE DISTANCE CHANGE STRATEGIES

The variation of the aforementioned maneuver reference yield different platooning strategies that allow to achieve trade-offs between the time and fuel consumption objectives. In this paper, we present three strategies: front, center and back references, further referred to as $r \in \{0, 0.5, 1\}$, respectively, in a platoon with an odd number of vehicles. This variable is used to find the reference vehicle index $i \in \mathcal{N}$ as $i = r \cdot (N_v - 1)$, with N_v the number of vehicles in the platoon. In the general case, the reference point is not restricted to a vehicle and can be placed anywhere in the Frenet-Serret frame. For example, when N_v is even, the reference point will be at the midpoint between the two middle vehicles.

2) DYNAMICS CONSTRAINTS

The vehicles in the platoon have inherent dynamical limitations, such as maximal speed and acceleration capabilities, arising from their mechanical properties. Additionally, we impose some maximal and minimal speeds around the target platoon speed using the speed deviation parameter, Δv . These parameters dictate the shape of the velocity profile during the maneuver in terms of height of the plateau. To reduce the complexity of the problem, we use symmetrical values around the target speed $v_g = 25$ m/s, $v_g \pm \Delta v$. A small speed operating area limits the consumption during the acceleration phase but yields a longer maneuver.

III. SIMULATION AND SCENARIOS

To compute the net fuel saving of an HDPL maneuver, we need to account for the IVD adaptation maneuvers. In this section, we present the method for studying the relationship between the duration and the fuel consumption of the maneuvers.

A fuel consumption model accounting for the reduced air drag is first derived from existing air drag models fitted to use fuel consumption inputs from SUMO. The computation of the two observed parameters, the fuel consumption and the duration of the maneuvers, is then provided. Finally, a scenario is implemented in order to collect the data that will be studied to derive the relationship between the two parameters.

A. FUEL CONSUMPTION MODEL FOR HDPL

The expected gain of truck platooning is a decreased overall fuel consumption. It is enabled by the reduced air drag experienced by each platoon member. Fuel consumption models integrated in microscopic vehicular simulator generally take into account individual vehicle parameters such as speed and acceleration. In a HDPL system, the air drag experienced by a truck is also strongly dependent on the other platoon members. As a result, we develop an air drag correction strategy, taking as inputs for each truck: (i) the fuel consumption considering individual air drag; (ii) the IVDs; and (iii) the position within the platoon.

We use a combination of the yaw averaged aerodynamic drag coefficient (YAD) mentioned in [25] and the non-linear air drag ratio ϕ , which derivation is presented in [26].

This non-linear, dimensionless, air drag ratio ϕ is at the essence of the fuel saving. $\phi(d) : \mathbb{R}_+ \rightarrow (0, 1]$ is a function of the IVD, but also considers the position of the vehicle within the platoon. $\phi \rightarrow 0$ when no drag force is experienced, $\phi = 1$ when the vehicle does not benefit from reduced air drag due to preceding trucks.

In [25], the YAD is expressed as:

$$\text{YAD} = \frac{\sum_{i=0}^{N_v-1} c_{D,i}^{\text{platooning}}}{\sum_{i=0}^{N_v-1} c_{D,i}^{\text{no-platoon}}}, \quad (3)$$

where c_D is the air drag coefficient, which is dimensionless. The term $c_{D,i}^{\text{platooning}}$ is equivalent to $c_{D,i}^{\text{no-platoon}} \phi(d)$ as the air drag ratio is correcting the air drag coefficient to reflect the effect of the preceding vehicles. Moreover, we consider a platoon of homogeneous trucks, as a result, $c_{D,i}^{\text{no-platoon}} = c_D$. Subsequently, eq. (3) becomes:

$$\begin{aligned} \text{YAD} &= \frac{\sum_{i=0}^{N_v-1} c_{D,i}^{\text{no-platoon}} \phi_i(d_i, v_i)}{\sum_{i=0}^{N_v-1} c_{D,i}^{\text{no-platoon}}} \\ &= \frac{c_D \sum_{i=0}^{N_v-1} \phi_i(d_i, v_i)}{N c_D} = \frac{1}{N} \sum_{i=0}^{N_v-1} \phi_i(d_i, v_i) = \bar{\phi}, \quad (4) \end{aligned}$$

where $\phi_i(d_i, v_i)$ is the air drag coefficient of the i -th truck having an IVD d_i and speed v_i , expressed in m and m/s

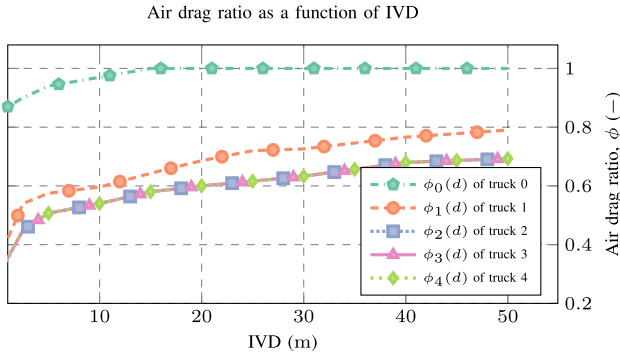


FIGURE 2. Air drag ratio as a function of IVD for five trucks in a platoon. We assume that the fourth and fifth trucks experience the same ratio as the third one. An air drag ratio of 1 corresponds to the truck driving alone, that is experiencing no advantage from other platooning trucks. Adapted from [26]. The first truck experiences a reduced air drag for short IVD due to non-laminar flow effects.

respectively. $\bar{\phi}$ denotes the average air drag coefficient to simplify the notation. $\phi_i(d_i)$ is obtained by matching the speed to the table of air drag ratios provided in [26] and is illustrated in Fig. 2. Note that thanks to the identification of $c_{D,i}^{\text{platooning}}$ and $c_{D,i}^{\text{no-platoon}}$ $\phi(d)$, the term c_D disappear from the YAD equation and is therefore not required anymore.

In [25], the estimated fuel saving is expressed as:

$$c^S = c^U \frac{1 - \bar{\phi}}{2}, \quad (5)$$

where c^S is the platoon fuel saving and c^U is the uncorrected platoon fuel consumption, which is the sum of the individual uncorrected fuel consumption of the platooning trucks, which we get from SUMO. The fuel consumption corrected by the estimated fuel saving c^C is therefore:

$$c^C = c^U + c^S = c^U \frac{\bar{\phi} + 1}{2}. \quad (6)$$

c^C , c^U and c^S are typically expressed in unit of volume per unit of time, typically in mL/s. In this paper, we are interested in the actual fuel saving of performing the HDPL maneuver. As a result, the savings that are computed are in comparison with not reducing the IVD, instead of just considering the correction factor (see Section III-B2).

B. METRICS

To maximize the efficiency of the platooning system, two metrics are accounted for: the duration of the closing and opening maneuvers, that also have to be minimized, as they reduce the amount of time the trucks are saving fuel during the fuel saving period, *viz.* when the trucks are driving with low IVD; the fuel consumption of the closing and opening maneuvers, that have to be minimize as they are deducted from the fuel saving of saving period. The two objectives are however concurrent, as faster maneuvers tend to be achieved by higher fuel consumption.

1) MANEUVER DURATION

We define the maneuver time T_m as the duration between the trigger of the IVD change (T_t) and the time at which the target is reached. This happens when:

$$\max(\zeta_i) \leq \epsilon,$$

where $\zeta_i = \overline{|s - b|}$ (see eq. (1)) for the local graph of node i and ϵ is a tolerance value, 1 m in the presented results. ζ_i is related to the mean deviation between the IVD and the target IVD for each vehicle. In other words, the maneuver duration is the time at which the state vector is equal to the bias vector and some tolerance.

2) FUEL CONSUMPTION IMPLEMENTATION

The fuel consumption of the maneuver C is the total relative fuel consumption of the platoon during the maneuver, calculated as a difference with the consumption of the same platoon not performing the maneuver. The baseline is obtained by simulating a platoon with the same input parameters, with no IVD adaptation. The relative fuel consumption C is therefore computed as:

$$c_k^U(t) = \sum_{i=0}^{N_v-1} c_{i,k}(t) \quad k \in \{m, b\} \quad (7)$$

$$c_k^C(t) = c_k^U(t) \frac{\bar{\phi} + 1}{2} \quad (8)$$

$$C_k = \int_0^{T_m} c_k^C(t) dt \quad (9)$$

$$C = C_m - C_b, \quad (10)$$

where $c_{i,k}(t)$ is the instantaneous fuel consumption of the truck i for the baseline ($k = b$) or the maneuver of interest ($k = m$). $c_{i,k}(t)$ is provided by the fuel consumption model of our traffic simulator SUMO, HBEFA3/HDV_TT, described in [27]. $c_k^U(t)$ is then the uncorrected instantaneous fuel consumption of the platoon and $c_k^C(t)$ the corrected instantaneous fuel consumption of the platoon. C_k is the total corrected fuel consumption over the duration of the maneuver of interest, T_m . Finally, C is the relative fuel consumption of the maneuver, expressed as the difference between the consumption of the maneuver and the consumption of the baseline (no maneuver). Instantaneous fuel consumptions $c_k^C(t)$ are expressed in unit of volume per unit of time and fuel consumptions C and C_k are expressed in unit of volume, typically mL/s and mL, respectively.

We investigate the gain of HDPL and compare different maneuvers by using the relative cost function as introduced in eq. (10). Using this model, we compute the net gain of performing HDPL with five trucks depending on the initial and final distances and report the results in Fig. 3. Particularly, the gain of performing HDPL at 5 m in comparison with platooning at 30 m is 2.2 mL/s with five trucks. These values will be used to calculate a compensation time, T_C , for the maneuver fuel investment in the next sections. This subsequently allows to transform fuel investments to compensation

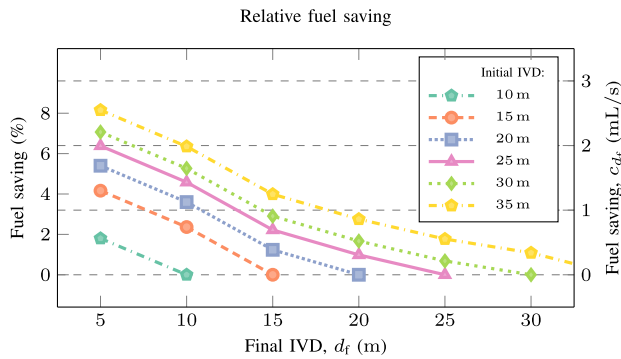


FIGURE 3. Fuel saving as a function of the final IVD for various initial IVDs. The saving is reported with respect to the same platoon not performing the IVD adaptation maneuver. It is expressed both in approximate relative value and absolute saving.

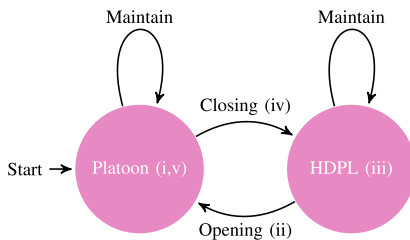


FIGURE 4. Finite-state diagram of the IVD adaptation process. In the presented simulation results, the closing and opening maneuvers are triggered at specific times in a standardized fashion in order to derive the fuel consumption and maneuver duration data. In the real setup, they are scheduled in the planning depending on the features of the PQoS time series.

times and *vice versa*. This is particularly useful when it comes to optimizing for both objectives: minimizing the fuel consumption and the maneuvering times.

C. SCENARIO

To observe the relationship between fuel consumption and maneuver duration, we consider a standardized platooning scenario on a closed circuit. This allows us to run the same scenario, independent on the actual maneuvering time, assuming that the platoon will achieve the formation changes in the imparted time. Our scenario is divided in five phases: (i) platooning; (ii) distance reduction; (iii) HDPL; (iv) distance augmentation and (v) platooning. We then assume that the platoon receives an information on a future favorable QoS and triggers the reduction of the distance (ii) in order to reduce the drag force experienced by the follower vehicles, aiming to reduce overall the fuel consumption. During the HDPL phase (iii), the platoon targets a new distance d_f . The platoon is then made aware of a degradation of the QoS and triggers the increase of the distance (iv). When the manoeuvre is achieved, that is when the IVD is back to its original value, the platoon continues to drive (v). The platoon is composed of five trucks, driving on the test circuit Ehra-Lessien, as illustrated in Fig. 5.

Fig. 4 illustrates the IVD adaptation process. In the study phase, the scenario is divided into three periods of 100 s: (i); (ii-iii); and (iv-v). The actual durations of the phases (ii)

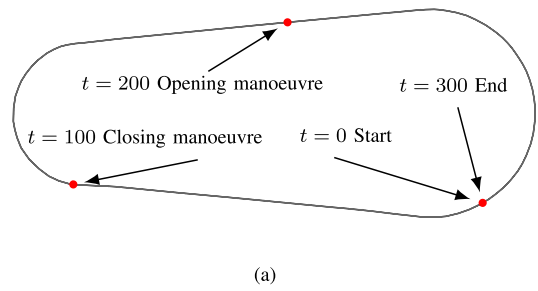


FIGURE 5. Scenario snapshots: (a) simulation model of Volkswagen Ehra-Lessien test track facility, and (b) zoom in on the five-truck platoon.

to (iv) depend on the maneuvering strategies implemented and are results of these experiments. In addition to enabling a standardized experimental process, the phases (i) and (iii) provide stabilization periods. The data gathered in this time-triggered implementation will allow to develop strategies to process actual PQoS time series. Each experiment indeed yields two maneuvering times and two maneuvering fuel consumptions.

Once the characteristics of the fuel consumption and maneuver duration are known, the trigger times of the closing and opening maneuvers are part of the optimization results. Their schedule will then depend on the features of the minimum IVD time series and therefore of the PQoS time series.

We run the HDPL scenario with a coupled traffic and network simulator, with SUMO [21] and ns-3 [22]. This combination has been chosen to leverage the link between platooning performance on the one side and QoS and surrounding traffic modeling on another side, as performed in the scope of the 5GNetMobil project, in which the work presented in this paper has been realized. We implement the control strategies described in the previous section directly in ns-3. Leveraging the tracing capabilities of ns-3, we gather instantaneous IVD, speed, fuel consumption and graph deviation time series for combinations of the control parameters. The rationale behind using a network simulator in this functional study is to enable running the fuel saving methods in the scope of framework including predictive communications algorithms, such as described in [18], in the future. The parameters for the communications systems are detailed in this paper.

D. SIMULATIONS

In the considered setup, the platoon behaviour is controlled by varying Δv , which defines its speed boundaries. With a low Δv , the platoon may reach its target formation faster, with the risk of consuming a large amount of fuel whilst maneuvering. With a larger Δv , it will benefit from the

TABLE 1. Simulation parameters.

Parameter	Notation	Values	Unit
Platoon speed	v_g	25	m/s
Reference	r	{0, 0.5, 1}	-
Speed boundaries	$v_g \pm \Delta v$	$v_g \pm \{1, 1.5, \dots, 3\}$	m/s
Initial IVD	d_i	{10, 15, 20, 25, 30}	m
Final IVD	d_f	{5, 10, 15, 20, 25}	m
Repetitions	-	3	-
Individual fuel consumption model	-	HBEFA3/HDV_TT	
Truck height	-	4	m
Truck width	-	2.55	m
Truck length	-	16.5	m

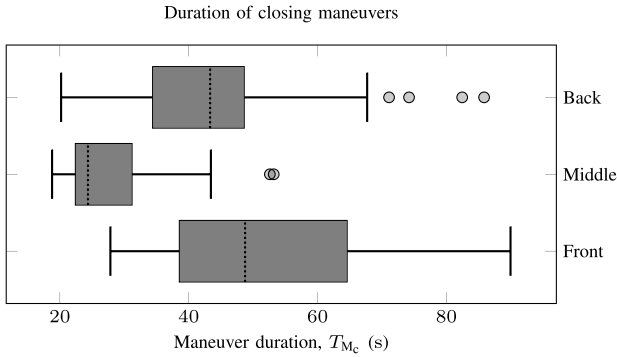


FIGURE 6. Duration of a closing maneuver for an initial IVD $d_i = 30$ m and a final IVD $d_f = 5$ m for the three maneuver references. The fastest maneuvers are achieved with the middle reference. The opening maneuver, which is not represented for clarity purposes, shows similar results.

reduced air drag for a shorter duration. To investigate the influence of the introduced references, we study multiple combinations of initial and final IVDs for varying speed boundaries. The simulated parameters are summarized in Table 1, yielding a total of 1500 experiments, including the baselines. We then process the obtained data time series in order to obtain the total fuel consumption and the maneuvering time. We choose to set the target platoon speed to 25 m/s = 90 km/h because it allows to provide a fair comparison with a realistic baseline. Indeed, multiple trucks driving with IVDs of 30 m at 90 km/h is a situation that can be observed on highways. It has the disadvantage of creating situations where the truck speed overreaches the maximum legal speeds in some countries. Considering that automated driving with IVDs of 5 m is also not yet allowed, these results are provided for the purpose of revealing the potential of HDPL. Lower target speeds have been investigated; the results are scaled down without drastic change in the tendencies. These results are not presented in this paper.

Figures 6 and 7 show the duration and the fuel consumption of closing maneuvers by the means of boxplots for the three studied references. The fastest maneuver can be achieved by setting the reference in the middle, but the lowest fuel consumption are achieved with the back reference. This illustrates that the choice of the reference is not trivial a compromise has to be found, balancing maneuver duration and fuel consumption.

Fig. 8 shows the two metrics as a function of the maximum speed deviation parameter for an illustrative scenario. The

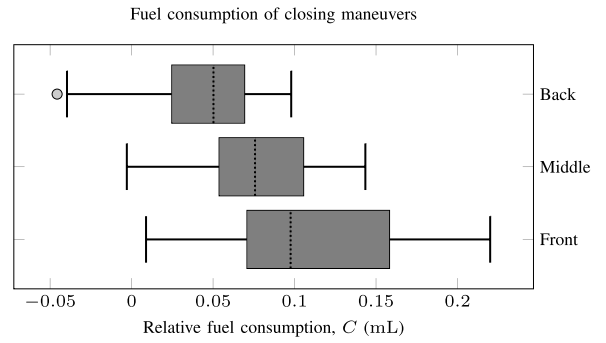


FIGURE 7. Fuel consumption of a closing maneuver for an initial IVD $d_i = 30$ m and a final IVD $d_f = 5$ m for the three maneuver references. The lowest relative fuel consumption are achieved with the back maneuver reference. The opening maneuver, which is not represented for clarity purposes, shows opposite results for the front and back references, which is explained by the symmetry of the maneuvers.

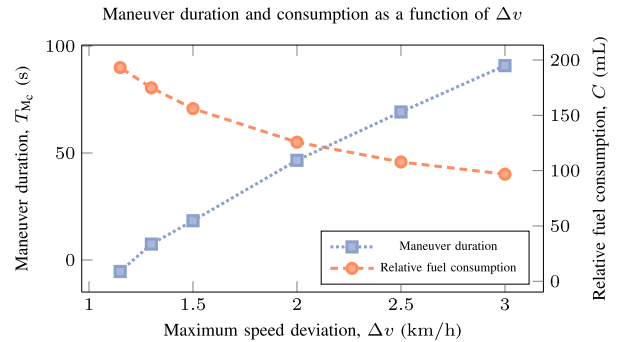


FIGURE 8. Influence of the maximum speed deviation parameter Δv (see Section II-B2) on the duration of the maneuver and the relative fuel consumption for an exemplary scenario. The maneuver duration can be reduced by allowing a larger maximum speed deviation, with the consequence, however, of increasing the fuel consumption. This illustrates the competing feature of the two objectives.

choice of this parameter also has a large impact on both metrics, with an opposite influence as a low maximum speed deviation yields a low fuel consumption and long maneuver, while a higher maximum speed deviation yields a high fuel consumption and a short maneuver.

maneuver and the fuel consumption of this maneuver using Δv .

E. MANEUVER PERFORMANCE MODELING

The previous results provide the maneuver duration and fuel consumption for discrete values of Δv , d_i and d_f . In order to use these results in an optimization framework, we first need to create a continuous model yielding the two metrics. This modeling has initial and final IVDs, a reference and a maximum speed deviation Δv as inputs. We choose to fit a least absolute shrinkage and selection operator (Lasso) model [28] to the obtained data. Lasso is a regression method that executes a variable selection and regularization step to improve the prediction accuracy. On top of the least square regression, Lasso constraints the sum of the coefficient absolute values under a threshold. As a result, the coefficients of the parameters with small or no influence on the predicted variable are set to zero or close to it. This constraint implements

both the regularization and the variable selection. Lasso is a univariate analysis method: The two observed variables, duration and relative fuel consumption, have therefore to be modeled separately.

We propose to take both the references (front—the state of the art—, middle and back) and the types of maneuver (opening and closing) into account by fitting six models (three maneuver references for each of the two maneuvers), and this for the two target values. This results in 12 regression models.

The inputs of these regressions are the initial and final IVDs, d_i and d_f respectively, and the speed boundaries Δv . Observing the shapes of the different points in the presented results, the target variables show a polynomial dependency on speed boundaries. Considering the regularization feature of the Lasso regression, we can take the polynomial combination of our features without risking over-fitting. To establish the degree of the polynomial combinations and the shrinking penalty λ , we perform an exhaustive grid search with k -fold cross validation. We use the coefficient of determination R^2 as scoring function and $k = 3$. If the degree of the polynomial is almost always 3 for the 12 models, the best value of λ is varying. This reinforces the motivation to use the grid search for all 12 models instead of fitting the hyper-parameters on one model only.

The obtained Lasso regressions allow us to obtain relative fuel consumption and maneuver durations for every combinations of maneuver (closing and opening), reference (front, middle, back) and initial and final distance, with $d_i \in [5, 30]$ m, $d_f \in [5, 30]$ m and $d_i > d_f$.

IV. FUEL CONSUMPTION OPTIMIZATION

Given the predicted values of a factor influencing the minimum IVD, we want to provide the best strategy for HDPL, accounting for the fuel consumption and the duration of the closing and opening maneuvers. The first step is to translate the predicted influencing factor values into a minimum allowed IVD considering the safety of the platoon. An example of such translation for PQoS is provided in [8] with the PIR as QoS indicator. This translation step allows to make the optimization framework independent of the chosen influencing factor. Moreover, IVD is part of the inputs of the models presented in the previous section, with d_i and d_f .

To simplify the usage of the aforementioned models, the provided times series of predicted influencing factor is simplified in the following way, with PIR as exemplary factor. The PIR is foreseen to suddenly drop (e.g., from 0.5 s to 0.05 s), to remain stable for a duration of T_F and then to increase back to its original value. In this example scenario, the future prediction of the PIR can either come from the network [3] or from a decentralized system [18]. The lower PIR value is finally translated into a minimum IVD, d_m . As a result, the provided input timeseries is modeled into a pair of values, a favorable time T_F and a minimum IVD allowance d_m .

The fuel saving optimization problem, which is constrained by this pair of values, is first presented. An evolutionary algorithm is then used to perform the optimization.

The aim is to choose a final IVD d_f and the corresponding r and Δv for the closing and opening maneuvers that maximize the fuel saving given the two constraints T_F and d_m . The platoon should only change its IVD to d_f , with $d_i > d_f \geq d_m$, if it is possible to execute the opening and closing maneuver and save fuel within a duration T_F . d_i denotes the initial IVD and is the IVD of the platoon before starting the maneuver. After the HDPL maneuver, the truck formation aims at returning to its initial state, with $d = d_i$.

The optimization problem can be formulated as:

$$\begin{aligned} \max \quad & F_S \\ \text{s.t.} \quad & d_i > d_f \geq d_m, \end{aligned} \quad (11)$$

where F_S is the effective fuel saving after deducing all maneuver consumptions. F_S is expressed in unit of volume.

To provide a solution to eq. (11), we need to investigate the dependency of F_S on the maneuvering parameters. F_S is a function of the effective fuel saving time T_H and the fuel saving rate c_{d_f} of the chosen target IVD d_f :

$$F_S = c_{d_f} T_H, \quad (12)$$

with $c_{d_f} = f(d_f)$, as illustrated in Fig. 3. c_{d_f} is in unit of volume per unit of time and T_H is in unit of time. The effective fuel saving time T_H is equal to the time during which the HDPL benefits from the small IVD. It takes all maneuver fuel consumption into account, *viz.* the consumption of the closing and opening maneuvers.

These maneuver consumptions are taken into consideration as compensation times for the opening and closing maneuvers. The compensation time corresponds to the time during which the HDPL has to maintain its target IVD to save enough fuel to compensate the fuel consumption of a maneuver. We denote the compensation time for closing and opening maneuvers as T_{C_c} and T_{C_o} , respectively. Both are obtained by dividing the maneuver relative fuel consumptions C by the fuel saving rate c_{d_f} , which depends on the chosen d_f :

$$T_C = \frac{C}{c_{d_f}}. \quad (13)$$

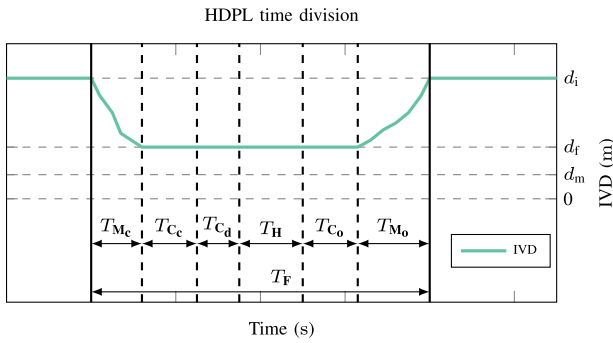
Accounting for the maneuvering times, we can express T_H as a function of the favorable time T_F :

$$T_H = T_F - T_{M_c} - T_{C_c} - T_{M_o} - T_{C_o} - T_{C_d}, \quad (14)$$

where T_{M_c} and T_{M_o} are the duration of the closing and opening maneuvers, respectively. The results presented in the previous section support that for some combinations of parameters, the compensation time can be null or negative. It is indeed possible to consume no fuel or even save fuel during maneuvers, in which case T_H includes part of the maneuvering time. Table 2 summarizes the different durations involved and Fig. 9 illustrates their dependence to IVDs.

TABLE 2. Time variables description in the optimization problem. The net duration of fuel saving is the favorable PQoS duration deducted by the maneuver durations and the compensation times.

Notation	Description
T_F	Favorable PQoS duration
T_{M_c}	Closing maneuver duration
T_{C_c}	Compensation time of the closing maneuver
T_{M_o}	Opening maneuver duration
T_{C_o}	Compensation time of the opening maneuver
T_{C_d}	Compensation time of the reference difference
T_H	Net duration of fuel saving


FIGURE 9. Illustrative representation of the IVD during the transformation between platooning to HDPL and return from HDPL to platooning. The IVD during closing and opening maneuvers, each maneuver compensation time as well as the fuel saving duration are represented.

To compute the relative fuel consumptions, we use a platoon not performing any maneuver as baseline. When the references for the opening and closing maneuvers are the same, the overall traveled distance remains identical to the baseline. However, when different references are used, this traveled distance differs and needs to be taken into consideration. Indeed, the platoon will consume fuel to travel a positive distance difference, or has saved fuel with a negative difference. To account for this additional fuel consumption or saving in our analysis, we introduce the traveled distance compensation time T_{C_d} . It corresponds to the time during which the HDPL has to maintain its target IVD to compensate the fuel consumed or saved because of the distance difference. T_{C_d} has the opposite sign of the distance difference. A negative T_{C_d} is then equivalent to extend T_H . T_{C_d} is computed as:

$$T_{C_d} = \frac{4(d_i - d_f)(r_o - r_c) \sum_{i=0}^5 c_{i,b|d=d_f}}{v_g c_{d_f}}, \quad (15)$$

where $c_{i,b|d=d_f}$ is the baseline instantaneous fuel consumption of the truck i at IVD $d = d_f$, and $r_c, r_o = \{0, 0.5, 1\}$.

From the results in the previous section, we know that the maneuvering times and the maneuvering fuel consumptions are dependent on the reference, the maximal speed deviation, the initial and final IVDs. T_{M_c} , T_{M_o} , T_{C_c} and T_{C_o} are therefore obtained from the models presented in Section III-E. The compensation times are dependent on the fuel consumptions and the fuel saving rate, which itself depends on the initial and final IVDs. We can therefore write the optimization

TABLE 3. Values and grid search intervals of PSO parameters.

Parameter	Value	Search interval
Number of particles	50	
Max number of iterations	1000	
Cognitive parameter		$[0.7, 3]$
Social parameter		$[0.7, 3]$
Inertia		$[0.7, 3]$

problem in the following form:

$$\begin{aligned} & \max_{\Gamma} F_S(\Gamma) \\ & \text{s. t. } d_i > d_f \geq d_m, \\ & \Gamma = (r_c, r_o, \Delta v_c, \Delta v_o, d_f), \end{aligned} \quad (16)$$

where the indices c and o correspond to the closing and opening maneuvers. Fixing d_i to the original target IVD of the platoon, we have five degrees of freedom in Γ .

V. OPTIMIZATION RESULTS

Given an influencing factor time series and its translation into a minimum IVD time series, we can describe this time series with two values, d_m and T_F . The objective function described in the previous paragraphs has the disadvantage of being non differentiable when considering the different references. This feature of the objective function prevents the use of any gradient-based method such as gradient descent and quasi-newton methods. To find the five parameters that maximize the fuel saving in eq. (16), we propose to use an intensive search optimization algorithm.

To present the optimization results, we choose PSO, an evolutionary algorithm that performs an iterative stochastic optimization [29], [30]. This choice is motivated by the relatively easy implementation of the problem in the optimization framework provided by `pyswarms` [31]. `pyswarms` offers a framework for using PSO adapted to constrained optimization problems by using a bounding box. It is however merely an example, this choice should be adapted to the available computing power.

We use a grid search based method for the hyper-parameter optimization including the boundaries of the particle speeds. Table 3 summarizes the values used for the swarm optimization and the grid search. We use the objective function as scoring method. We apply the grid search to several combinations of favorable duration, T_F , initial IVD, d_i and minimum IVD. The chosen hyper-parameter tuple is the one that makes PSO yield the best solution the most frequently.

With this setup implemented on a simple desktop computer, the algorithm converges in a few seconds. The grid search requires more time, in the order of magnitude of the day, but should only be run once to get the optimal hyper-parameters. As mentioned earlier, the PSO setup is not meant to be used in a real-world deployment, but to provide the results in the following.

Our ultimate goal is to choose a set of parameters for the closing and the opening maneuvers that will maximize the fuel saving, and, in turns, to derive the prediction horizon

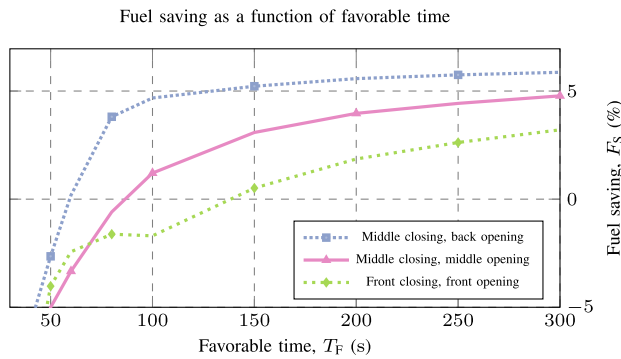


FIGURE 10. Fuel saving in percentage as a function of the favorable time for a minimum IVD of $d_m = 5$ m for representative combination of maneuver references. The highest saving is obtained for the middle reference closing maneuver and back reference opening maneuver. The classical front references are performing the worst.

value. To do so, we perform the optimization with different sets of T_F and d_m . We can then observe the fuel saving as a function of T_F for different values d_m and obtain an order of magnitude of the prediction horizon.

Fig. 10 shows the results of the fuel saving optimization with a minimum IVD $d_m = 5$ m and an initial IVD $d_i = 30$ m. Here, 5 m is the minimum constraint, the platoon can target any IVD between d_m and d_i . We actually force the platoon to perform a maneuver by reducing the upper bound to 25 m. We can observe that the maximal fuel saving is generally achieved by a combination of the middle closing and back opening maneuvers. Indeed, the platoon reaches an optimum by quickly closing the gap and then opening it slower to maximize the benefit of HDPL.

We also observe that the fuel saving becomes positive between 80 s to 150 s depending on the strategy combination. Generally, all strategies outperform the classical approach with front reference for all maneuvers. Finally, all curves tend to a plateau. This plateau represents the maximal fuel saving in percentage, which is reached when the maneuver costs become negligible compared to the fuel saved at low IVD. For the best performing set of maneuvers, it is reached around $T_F = 200$ s. This means that, at 90 km/h, a platoon needs to drive 5 km before the maneuver costs become negligible. The worst performing set of maneuvers reaches this plateau at 600 s (not represented for clarity purposes in Fig. 10), which corresponds to driving 15 km.

Fig. 11 presents the corresponding target IVD. For the most fuel-efficient strategies, d_m is reached with T_F around 100 s. For the case of the classical front reference approach a favorable period of 300 s is required. Under 100 s, combinations involving the front opening maneuver have the maximal IVD as target.

One can choose the prediction horizon by choosing an appropriate level of achievable fuel saving and the corresponding necessary favorable time, as presented in Fig. 10 for instance. Indeed, the future conditions need to be predicted in order to determine if the platoon can drive lower inter-vehicle distance. In this choice, one has to also take

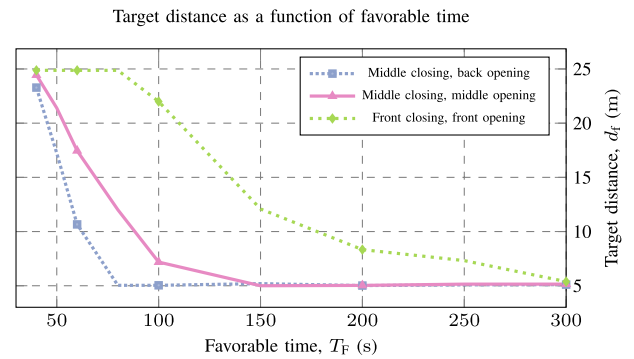


FIGURE 11. Target IVD d_t as a function of the favorable time for a minimum IVD of $d_m = 5$ m for representative combination of manoeuvre references.

into account the target IVD, as the prediction horizon also influences the confidence in the predicted value, meaning that lower IVDs are more difficult to predict in a further future.

100 s is the order of magnitude of the prediction horizon requirement. As mentioned in the introduction, one example of influencing factor is PQoS. For a prediction system of a decentralized communications system such as the one described in our previous work [18], this might be challenging as the prediction requires the future position of the surrounding communicating vehicles. Accurately predicting the position of vehicles 100 s is indeed a difficult task. Depending on the accuracy requirement of the prediction system, this task can be eased by the broadcasting of vehicles trajectory. Another solution is to rely on a cellular communications system which proposed a PQoS feature, such as 5G, which promises it in future releases.

These results are closely bound to the chosen target speed of 90 km/h. Reducing this target speed, the gain from reduced air drag is first limited as it is proportional to the absolute fuel consumption. Moreover, the closing and opening maneuvers would be longer as the mobility rapidity of trucks is reduced; as a result, for a given prediction horizon, the platoon would either target a larger IVD or a benefit from this target IVD for a shorter time.

VI. CONCLUSION

In this paper, we study manoeuvring strategies to achieve fuel efficiency while doing truck high density platooning. We introduce the concept of reference placement in a truck platoon control system to balance between the two objectives of this problem: the fuel consumption and the duration of the maneuver minimizations. We study the relationship between these two metrics as a function of different maneuver parameters.

This study not only considers the fuel saving achieved by driving small headways but also during the maneuvers by developing a fuel consumption correction method. We show that some strategies achieve fuel saving while performing the maneuver, at a cost of longer maneuvering durations. The

correction model also allows us to link the fuel consumption of the maneuver with a compensation time.

Using these results, we are able to compute the required prediction horizon for a predictive quality of service system. This time is dependent on how far in the future the favorable quality of service will occur, as it drives the minimum maneuvering time. We present the application of this prediction horizon derivation on a packet inter-reception time prediction time series that is translated into a minimum inter-vehicle distance time series. We first show that changing the reference of the maneuvers enables higher fuel savings. We show that in order to actually achieve fuel efficiency with a minimum IVD of 5 m, a platoon requires a projection of around 60s in the future, considering that the quality of service is provided without any cost.

These results provide the prediction horizon requirements for prediction mechanisms in the scope of truck high-density platooning systems. Linked with a system providing the feasible inter-vehicle distance considering the future quality of service, this decision making strategy will be an enabler for agile quality of service adaptation.

The framework presented in this paper will also be used to study the behavior of the prediction horizon and of the target inter-vehicle distance with respect to different target speeds and platoon sizes. As the traffic density can be predicted and then translated into future conditions, this will allow to provide an extensive study of the feasibility of truck high-density platooning in various external conditions.

APPENDIX

In this example illustrating the maneuver reference, we consider a three-vehicle platoon having IVDs of 10 m and 5 m at a certain timestep, targeting an IVD of 8 m. For the sake of simplicity, we assume that there is a communication link between each pair of vehicles, which results in the Laplacian being equal to 1. The vehicle length is 2 m. As a result, eq. (2) becomes:

$$\dot{s} = -1 \cdot (s - b) + v_g. \quad (17)$$

The target time derivative of the state vector \dot{s} is calculated for three cases:

- 1) front reference \dot{s}_0 ;
- 2) middle reference $\dot{s}_{0.5}$;
- 3) and back reference \dot{s}_1 .

A. FRONT REFERENCE

With the first truck as front reference, the state and bias vectors are:

$$s_0 = \begin{bmatrix} 0 \\ -(10 + 2) \\ -(10 + 2 + 7 + 2) \end{bmatrix} \quad (18)$$

$$b_0 = \begin{bmatrix} 0 \\ -10 \\ -20 \end{bmatrix}. \quad (19)$$

The resulting \dot{s}_0 is finally obtained using eq. (17):

$$\begin{aligned} \dot{s}_0 &= s_0 - b_0 + v_g \\ &= - \left(\begin{bmatrix} 0 \\ -12 \\ -21 \end{bmatrix} - \begin{bmatrix} 0 \\ -10 \\ -20 \end{bmatrix} \right) + 25 = \begin{bmatrix} 25 \\ 27 \\ 26 \end{bmatrix}. \end{aligned} \quad (20)$$

B. MIDDLE REFERENCE

In this case, the vectors are:

$$s_{0.5} = \begin{bmatrix} 12 \\ 0 \\ -9 \end{bmatrix} \quad (21)$$

$$b_{0.5} = \begin{bmatrix} 10 \\ 0 \\ -10 \end{bmatrix}. \quad (22)$$

We then obtain

$$\dot{s} = \begin{bmatrix} -2 \\ 0 \\ -1 \end{bmatrix} + 25 = \begin{bmatrix} 23 \\ 25 \\ 24 \end{bmatrix}. \quad (23)$$

C. BACK REFERENCE

Using the same logic with the last truck as reference:

$$\dot{s} = - \left(\begin{bmatrix} 21 \\ 9 \\ 0 \end{bmatrix} - \begin{bmatrix} 20 \\ 10 \\ 0 \end{bmatrix} \right) + 25 = \begin{bmatrix} 24 \\ 26 \\ 25 \end{bmatrix}. \quad (24)$$

D. INTRODUCING Δv

We already see that, depending on the reference in this rather simple case, the target speed distribution changes. Driving with higher speed generally increase the fuel consumption. Another parameter of the system is the maximum deviation from the target speed v_g , which may reduce the target speed in certain case and therefore the fuel consumption, but in turns lead to longer convergence of the formation. In this example, $v_g = 25$ m/s. Applied to the previous value, the new target speed vectors are:

$$\dot{s}_0 = \begin{bmatrix} 25 \\ 26 \\ 26 \end{bmatrix}, \quad (25)$$

$$\dot{s}_{0.5} = \begin{bmatrix} 24 \\ 25 \\ 24 \end{bmatrix}, \quad (26)$$

$$\dot{s}_1 = \begin{bmatrix} 24 \\ 26 \\ 25 \end{bmatrix}. \quad (27)$$

The parameter Δv has an influence on both the fuel consumption and the maneuver duration, and can therefore be used to balance between the two objectives. In some cases, this speed limitation may result in the algorithm not converging. The simulated scenarios are however not concerned by this issue.

REFERENCES

- [1] A. Al Alam, A. Gattami, and K. H. Johansson, "An experimental study on the fuel reduction potential of heavy duty vehicle platooning," in *Proc. 13th Int. IEEE Conf. Intell. Transp. Syst. (ITSC)*, 2010, pp. 306–311.
- [2] S. Tsugawa, S. Jeschke, and S. E. Shladover, "A review of truck platooning projects for energy savings," *IEEE Trans. Intell. Veh.*, vol. 1, no. 1, pp. 68–77, Mar. 2016.
- [3] A. Kousaridas *et al.*, "QoS prediction for 5G connected and automated driving," *IEEE Commun. Mag.*, vol. 59, no. 9, pp. 58–64, Sep. 2021.
- [4] L. Zhang, F. Chen, X. Ma, and X. Pan, "Fuel economy in truck platooning: A literature overview and directions for future research," *J. Adv. Transp.*, vol. 2020, Jan. 2020, Art. no. 2604012. [Online]. Available: <https://www.hindawi.com/journals/jat/2020/2604012/>
- [5] B. McAuliffe, M. Lammert, X.-Y. Lu, S. Shladover, M.-D. Surcel, and A. Kailas, "Influences on energy savings of heavy trucks using cooperative adaptive cruise control," SAE, Warrendale, PA, USA, Rep. 2018-01-1181, 2018.
- [6] S. Torabi and M. Wahde, "Fuel-efficient driving strategies for heavy-duty vehicles: A platooning approach based on speed profile optimization," *J. Adv. Transp.*, vol. 2018, Sep. 2018, Art. no. 4290763.
- [7] M. Di Bernardo, A. Salvi, and S. Santini, "Distributed consensus strategy for platooning of vehicles in the presence of time-varying heterogeneous communication delays," *IEEE Trans. Intell. Transp. Syst.*, vol. 16, no. 1, pp. 102–112, Feb. 2015.
- [8] A. Pfadler, G. Jornod, A. El Assaad, and P. Jung, "Predictive quality of service: Adaptation of inter vehicle distance to packet inter-reception time for HDPL," in *Proc. IEEE 91st Veh. Technol. Conf. (VTC Spring)*, 2020, pp. 1–5.
- [9] M. E. Renda, G. Resta, P. Santi, F. Martelli, and A. Franchini, "IEEE 802.11p VANets: Experimental evaluation of packet inter-reception time," *Comput. Commun.*, vol. 75, pp. 26–38, Feb. 2016.
- [10] S. van de Hoef, K. H. Johansson, and D. V. Dimarogonas, "Fuel-efficient en route formation of truck platoons," *IEEE Trans. Intell. Transp. Syst.*, vol. 19, no. 1, pp. 102–112, Jan. 2018.
- [11] C. Zhai, Y. Liu, and F. Luo, "A switched control strategy of heterogeneous vehicle platoon for multiple objectives with state constraints," *IEEE Trans. Intell. Transp. Syst.*, vol. 20, no. 5, pp. 1883–1896, May 2019.
- [12] G. Guo and Q. Wang, "Fuel-efficient en route speed planning and tracking control of truck platoons," *IEEE Trans. Intell. Transp. Syst.*, vol. 20, no. 8, pp. 3091–3103, Aug. 2019.
- [13] C. Zhai, F. Luo, Y. Liu, and Z. Chen, "Ecological cooperative look-ahead control for automated vehicles travelling on freeways with varying slopes," *IEEE Trans. Veh. Technol.*, vol. 68, no. 2, pp. 1208–1221, Feb. 2019.
- [14] V. Turri, B. Besselink, and K. H. Johansson, "Cooperative look-ahead control for fuel-efficient and safe heavy-duty vehicle platooning," *IEEE Trans. Control Syst. Technol.*, vol. 25, no. 1, pp. 12–28, Jan. 2017.
- [15] G. Jornod, T. Nan, M. Schweins, A. El Assaad, A. Kwoczek, and T. Kürner, "Sideline technologies comparison for highway high-density platoon emergency braking," in *Proc. IEEE 16th Int. Conf. Intell. Transp. Syst. Telecommun. (ITST)*, Oct. 2018, pp. 1–7.
- [16] G. Jornod, R. Alieiev, A. Kwoczek, and T. Kürner, "Environment-aware communications for cooperative collision avoidance applications," in *Proc. IEEE 19th Int. Symp. World Wireless Mobile Multimedia Netw. (WoWMoM)*, Jun. 2018, pp. 588–599.
- [17] R. Alieiev, G. Jornod, T. Hehn, A. Kwoczek, and T. Kürner, "Improving the performance of high-density platooning using vehicle sensor-based doppler-compensation algorithms," *IEEE Trans. Intell. Transp. Syst.*, vol. 21, no. 1, pp. 421–432, Jan. 2020.
- [18] G. Jornod, A. E. Assaad, and T. Kürner, "Packet inter-reception time conditional density estimation based on surrounding traffic distribution," *IEEE Open J. Intell. Transp. Syst.*, vol. 1, pp. 51–62, 2020.
- [19] G. Jornod, "Predictive vehicle-to-vehicle communications for fuel-efficient platooning," Ph.D. dissertation, Dept. Institut für Nachrichtentechnik, Technische Universität Braunschweig, Braunschweig, Germany, 2021.
- [20] I. Navarro, F. Zimmermann, M. Vasic, and A. Martinoli, "Distributed graph-based control of convoys of heterogeneous vehicles using curvilinear road coordinates," in *Proc. 19th IEEE Int. Conf. Intell. Transp. Syst. (ITSC)*, 2016, pp. 879–886.
- [21] P. A. Lopez *et al.*, "Microscopic traffic simulation using SUMO," in *Proc. 21st IEEE Int. Conf. Intell. Transp. Syst.*, 2018, pp. 2575–2582.
- [22] G. F. Riley and T. R. Henderson, *The NS-3 Network Simulator*. Heidelberg, Germany: Springer, 2010, pp. 15–34. [Online]. Available: https://link.springer.com/chapter/10.1007/978-3-642-12331-3_2#citeas
- [23] I. Llatser, G. Jornod, A. Festag, D. Mansolino, I. Navarro, and A. Martinoli, "Simulation of cooperative automated driving by bidirectional coupling of vehicle and network simulators," in *Proc. IEEE Intell. Veh. Symp. (IV)*, 2017, pp. 1881–1886.
- [24] M. Mesbahi and M. Egerstedt, *Graph Theoretic Methods in Multiagent Networks*, vol. 33. Princeton, NJ, USA: Princeton Univ. Press, 2010.
- [25] P. Vegendla, T. Sofu, R. Saha, M. M. Kumar, and L.-K. Hwang, "Investigation of aerodynamic influence on truck platooning," SAE, Warrendale, PA, USA, Rep. 2015-01-2895, 2015.
- [26] H. Wolf-Heinrich and S. R. Ahmed, *Aerodynamics of Road Vehicles*. Warrendale, PA, USA: Soc. Autom. Eng., 1998.
- [27] S. Hausberger and D. Krajzewicz, "COLOMBO deliverable 4.2: Extended simulation tool PHEM coupled to SUMO with user guide," document FP7-ICT-2011-8, DLR, Berlin, Germany, Feb. 2014.
- [28] R. Tibshirani, "Regression shrinkage and selection via the lasso," *J. Royal Stat. Soc. Series B*, vol. 58, no. 1, pp. 267–288, 1996.
- [29] J. Kennedy and R. Eberhart, "Particle swarm optimization," in *Proc. Int. Conf. Neural Netw. (ICNN)*, vol. 4, Nov. 1995, pp. 1942–1948.
- [30] Y. Shi and R. Eberhart, "A modified particle swarm optimizer," in *Proc. IEEE Int. Conf. Evol. Comput.*, May 1998, pp. 69–73.
- [31] L. J. V. Miranda, "PySwarms, a research-toolkit for particle swarm optimization in Python," *J. Open Source Soft.*, vol. 3, no. 21, p. 433, 2018. [Online]. Available: <https://doi.org/10.21105/joss.00433>



GUILLAUME JORNOD received the B.Sc. and M.Sc. degrees in environmental science and engineering (ing. env. dipl. EPF) from the École polytechnique fédérale de Lausanne (EPFL), Switzerland, in 2012 and 2014, respectively, the M.Sc. degree in management from the University College London, U.K., in 2015, and the Ph.D. degree in vehicle-to-vehicle communications in conjunction from the Technische Universität Braunschweig, in 2020, under the supervision of Prof. Dr.-Ing. T. Kürner.

From 2015 to 2017, he was with the Distributed Intelligent Systems and Algorithms Laboratory, EPFL, with Prof. Martinoli, where he was a Research and Development Engineer and was involved in the distributed control algorithm integration and deployment for the FP7 project AutoNet 2030. From 2017 to 2020, he was with the Cooperative systems and Communications Technologies Department, Volkswagen Group Research, Wolfsburg, Germany. In 2020, he joined the program Digital Rail Germany within DB Netz AG, Berlin, Germany, as 5G Communications Expert, where he is involved in specifications for Future Railway Mobile Communication System and in the European project 5GRail.



ANDREAS PFADLER received the M.Sc. degree in telecommunication engineering with specialization in wireless communications from the Polytechnic University of Catalonia, Barcelona, Spain, in 2018. He is currently pursuing the Ph.D. degree in vehicular communications with the Technische Universität of Berlin, under the supervision of Prof. Dr.-Ing. S. Stanczak. He is a Communication Expert and Function Developer of Automated Driving with Volkswagen Commercial Vehicles.

He is involved in several research projects as the European project 5GCroCo and the German national project 5G NetMobil. His research interests include antenna design, signal processing, predictive quality of service, new waveforms, and wave propagation.



SOFIA CARREIRA received the B.Sc. and M.Sc. degrees in mechanical engineering with specialization in control systems and computational intelligence from the Instituto Superior Técnico (IST), University of Lisbon, Portugal. In 2019, she was intern with the Cooperative Systems and Communications Technologies Department, Volkswagen Group Innovation, Wolfsburg, Germany. In 2020, she joined IS4 the Laboratory of Intelligence Systems for Data Analysis, Modeling and Optimization, IST, where her

research connects machine learning with healthcare treatment in the ICU. In October 2021, she joined the Platform Integration Automated Driving Department, Mercedes-Benz AG, Stuttgart, Germany.



AHMAD EL ASSAAD received the Dipl.-Ing. degree in electrical engineering and information technology from RWTH Aachen University, Germany, in 2012, and the Ph.D. degree in traffic telematics from the Technical University of Dresden, Germany, in 2021. From 2012 to 2017, he was a Research and Development and a Software Engineer with Elektrobit Automotive GmbH, Laird and Continental Automotive. He developed V2X applications for autonomous parking, systems for simultaneous precise mobile

positioning and mobile communications in connected driving, and localization systems of smartphones outside and inside of vehicles for smart vehicle access. He joined the Cooperative and Communications Technologies Department, Volkswagen Group Innovation, Wolfsburg, Germany, from April 2017 until March 2020. His research scope included hybrid communications systems, 5G-NR V2X and predictive quality of service for connected and automated driving. From April 2020 to June 2021, he managed a simultaneous engineering team for the deployment of infotainment and connected cars technologies at Volkswagen Commercial Vehicles, Wolfsburg. Since July 2021, he has been responsible for the coordination of technology modules for connected cars and mobile online services with Volkswagen AG, Wolfsburg.



THOMAS KÜRNER (Fellow, IEEE) received the Dipl.-Ing. degree in electrical engineering and the Dr.-Ing. degree from the University of Karlsruhe, Germany, in 1990 and 1993, respectively. From 1990 to 1994, he was with the Institut für Höchstfrequenztechnik und Elektronik, University of Karlsruhe working on wave propagation modeling, radio channel characterization and radio network planning. From 1994 to 2003, he was with the Radio Network Planning Department at the headquarters of the GSM 1800 and UMTS

operator E-Plus Mobilfunk GmbH & Co KG, Düsseldorf, where he was team manager radio network planning support responsible for radio network planning tools, algorithms, processes and parameters from 1999 to 2003. Since 2003, he has been a Full University Professor of Mobile Radio Systems with the Technische Universität Braunschweig. In 2012, he was a Guest Lecturer with Dublin City University within the Telecommunications Graduate Initiative in Ireland. He is also the Project Coordinator of the H2020-EU-Japan project ThoR (TeraHertz End-To-End Wireless Systems Supporting Ultra-High Data Rate Applications) and a Coordinator of the German DFG-Research Unit FOR 2863 Meteracom (Metrology for THz Communication). He is currently chairing the IEEE 802.15 Standing Committee THz. He was also the Chair of IEEE 802.15.3d TG 100G, which developed the worldwide first wireless communications standard operating at 300 GHz. In 2019, he received the Neal-Shephard Award of the IEEE Vehicular Technology Society. From 2016 to 2021, he was a Member of the Board of Directors of the European Association on Antennas and Propagation and since 2020, he has been a Distinguished Lecturer of IEEE Vehicular Technology Society.